Numerical simulations on the performance of FAPbI₃ based solar cell with CDS as buffer layer

Roshan G V S Bommidi[a*], Sreedhar Karakavalasa [a*], Sridhar Bendi[a*]

[a]Basic Sciences and Humanities Department, Aditya Institute of Technology and Management, K. Kotturu, Tekkali 532201, Srikakulam District, Andhra Pradesh, India.
*All authors carry equal contribution to the present work
*Author for Correspondence

Abstract
This study investigates the performance optimization of FAPbI₃-based perovskite solar cells incorporating Cu₂O as the hole transport layer (HTL), ZnSnO (ZTO) as the electron transport layer (ETL), and CdS as a buffer layer between the perovskite and ETL. Device performance is shown to be highly sensitive to the thickness of the perovskite layer. Optimal thickness (~400–500 nm) maximizes light absorption, leading to increase short-circuit current density (Jsc), while mitigating recombination losses. Open-circuit voltage (Voc) decreases with increasing thickness due to quasi-Fermi level splitting reduction. Fill factor (FF) peaks at intermediate thicknesses (~300–400 nm), balancing resistive and recombination losses. The overall power conversion efficiency (PCE) follows the trends of Jsc and FF, peaking at optimal thickness. The inclusion of CdS as a buffer layer significantly reduces interfacial recombination, enhancing charge transport and stability. This work highlights the critical role of thickness optimization and interfacial engineering in advancing the scalability and efficiency of perovskite solar cells.
Keywords: Formamidinium Lead Iodide (FAPbI₃), Perovskite Solar cell, Simulation, Numerical Simulation.

I.   Introduction

Over the past few decades, silicon is the key player in commercial solar cell technology. But, the energy sector always demands for the new materials for future technology without much compromising with the efficiency/ properties. Hybrid perovskite solar cells, because of their many sided advantages have a great chance as a successor for industrial applications. MAPbI₃, a prototype in perovskite solar cells achieved a PCE of around 25% so far. One of the major setbacks for MAPbI₃ is their absorption limit in NIR region to reach Shockley-Queisser limit [1]. This issue has been circumvented by replacing the MA⁺ cation with FA⁺ as pristine α-FAPbI₃ offers relatively lower volatility and higher thermal stability as well as the optical band edge nearing to 1.47 eV extending the light absorption into near IR region. With this band gap of 1.47 eV, FAPbI₃ can serve as an ideal candidate for single junction solar cells. Although the band gap of MAPbI₃ can be tuned from 1.55 to 2.3 eV with varying the halide composition between iodide and bromide for applications in multi junction solar cells, the light absorption cannot be increased in the near IR with this composition [2]. Therefore, studies on solar cells fabricated with pristine α-FAPbI₃ draws major attention. However, FAPbI₃ transforms itself from photoactive black α-phase to the photo inactive yellow δ-phase below 150°C. This problem can be overcome by replacing cation/anion sites with MA, Cs or Br ions. But, this partial replacement of anions or cations triggered other issues such as low thermal stability caused by the presence of mixed halides and reduced photon absorption resulting in low current density owing to an undesirable increase in the band gap. The comparisons between the experimental and numerical simulated photovoltaic characteristics of pristine α-FAPbI3 were studied and reported [3]. They used the experimentally obtained thickness for ETL, HTL and perovskite active layers as well as E_g values of these absorber layers as input parameters in SCAPS 1D. The efficiency is reported to be ~21.4% and 4.3% for the simulated and experimental respectively. They attributed this major transition in PCE's to the spontaneous and rapid transition from the optically active α-phase (black) to the inactive δ-phase (yellow) in deposited films.

From molecular dynamics (MD), it was inferred that FA reorientation was faster than MA on the A-cation site of the perovskite, which led to enhanced stabilization and slower charge carrier recombination [4]. This work accounted for an PCE of > 23% for α-FAPbI₃ films prepared using FASCN vapor assisted treatment and tested the long term operational stability (under 500 h of MPP tracking) and PCE is found to be remained at ~90% of the initial value (21.4%). A study on the effect of methylenediammonium dichloride (MDACl₂) doped α-FAPbI₃ films achieved a certified PCE of 23.7% and this value has been retained close to 90% under 600 h of

operation under full sunlight illumination in ambient conditions including UV light [5]. A report on the effect of cationic and anionic additives in FAPbI₃ on their PV parameters interestingly found that PCE got significantly improved from 16.55 to 22.51% in case of Cl⁻ (20%) addition in α-FAPbI₃ without shift in absorption edge from the pristine [6]. In addition, they noticed higher absorbance for FACl (20%) than α-FAPbI₃. This is due to the chloride in FACl used as an additive was found on grain boundary rather than in the grains, which eventually has positive effect on passivating iodide-deficient grain boundary.

In this regard, there is always a quest in exploring the better ways of enhancing the efficiency of FAPbI₃ based solar cells with varying configurations/additives in α-FAPbI₃. Choice of electron transport layer is very crucial for better performance in minimizing the interfacial defects through trap states. Over the time, the combination of PSCs with TiO₂ as ETL is in high demand. Although TiO₂ is the most widely utilized ETL, it still presents some electronic and optical shortfalls. Due to deficiencies such as low electron mobility, high defect states at the TiO₂/perovskite interface, insufficient band offset, requirement of high sintering temperature and degradation of perovskite materials under light illumination in the presence of TiO₂ owing to its photo catalytic properties, great attention has been drawn to find alternative ETL materials. Ternary metal oxide materials like Zn₂SO₄ (ZTO), SrTiO₃ and BaSnO₃ appear to be attractive compared to binary oxides like ZnO and SnO₂. ZTO has a small electron effective mass of 0.23 me, high electron mobility (10-30 cm²V⁻¹s⁻¹), high electrical conductivity, wide optical band gap (3.8 eV) and a suitable conduction band edge resulting in fast charge injection collection from perovskite. Although ZTO is being studied as an alternative to TiO₂, so far the device performance of PSCs with ZTO is still lower compared with TiO₂ ETLs. Therefore, further studies are needed to significantly improve the performance of PSCs with ZTO [7].

As a promising and widely used material in PV devices, CdS possesses a good band level between FTO and the perovskite. The main objective of the research here in is to optimize the perovskite/CdS thin film solar cell (TFSC) for the best PCE by varying the layer parameters and operating conditions of the solar cell. The present study focuses on an alternative for electron extraction interlayer, based on the CdS as an interlayer to enable better charge transfer from perovskite into the electron extraction layer.

Fig.1: Cell configuration for simulated thin film solar cell

II.   Numerical simulation and modeling parameters

All numerical simulations were carried out using Solar Cell Capacitance Simulator (SCAPS-1D) software, a one-dimensional solar cell simulation program developed by Dr. Marc Burgelman and his team at department of Electronics and Information systems of the University of Gent, Belgium. The main functionality of SCAPS is to solve the one-dimensional semiconductor equations to model thin film solar cells. In the bulk of the layers these equations are given by Poisson's equations along with carrier continuity equations (1) as mentioned below together with the constitutive equations (2)

$$\frac{\partial n}{\partial t} = G_n - U_n + \frac{1}{q} \nabla . J_n$$

$$\frac{\partial p}{\partial t} = G_p - U_p - \frac{1}{q} \nabla.J_p$$

Where G_n and G_p are the electron and hole generation rate (cm^{-3}-s^{-1}) respectively, caused by external influences such as the optical excitation with photons or impact ionization under large electric fields. The recombination rates can be given by

$$U_n = \frac{\Delta n}{\tau_n} \text{ and } U_p = \frac{\Delta n}{\tau_p}$$

For the one-dimensional case under a low injection condition, the above equation reduce to

$$\frac{\partial n_p}{\partial t} = G_n - \frac{n_p - n_{po}}{\tau_n} + n_p \mu_n \frac{\partial E}{\partial x} + \mu_n E \frac{\partial n_p}{\partial x} + D_n \frac{\partial^2 n_p}{\partial x^2}$$

$$\frac{\partial p_n}{\partial t} = G_p - \frac{p_n - p_{no}}{\tau_p} - p_n \mu_p \frac{\partial E}{\partial x} - \mu_p E \frac{\partial p_n}{\partial x} + D_p \frac{\partial^2 p_n}{\partial x^2}$$

The above set of equations is solved numerically to extract the required solar parameters.

In the present study, One-dimensional planar n-i-p configuration (FTO/Zn₂SO₄/CdS/FAPbI₃/Cu₂O/Au) was used for simulation by SCAPS 1D. The CdS used as an n-type buffer layer which can be considered as a hole blocking layer.

Table 1: Input parameters of different layers used in SCAPS-1D simulation tool for the present study

Parameters	FTO	Zn₂SO₄	CdS	FAPbI₃	Cu₂O
Thickness (nm)	400	250	250	100-900	300
Bandgap (eV)	3.5	3.5	2.4	1.51	2.17
Electron Affinity (χ)	4.0	4.0	4.0	4.0	3.2
Permittivity	9.0	9.0	10.0	6.6	7.1
Effective density of states at CB (/cm^3)	2.02E+18	2.2E+18	2.2E+18	1.2E+19	2.5E+18
Effective density of states at VB (/cm^3)	1.8E+19	1.8E+19	1.8E+19	2.9E+18	1.8E+19
e^- thermal velocity	1E+7	1E+7	1E+7	1E+7	1E+7
h^+ thermal velocity	1E+7	1E+7	1E+7	1E+7	1E+7
Mobility of e^-	2E+2	3.2E+8	1E+2	2.7E+2	2.0E+2
Mobility of h^+	1E+1	5E+1	2.5E+1	1.8E+0	8E+1
Density of n-type doping (/cm^3)	2E+19	1E+19	0	1.3E+16	0
Density of p-type doping (/cm^3)	0	1E+0	1E+18	1.3E+16	9E+21
Density of defects (/cm^3)	1E+15	1E+15	1E+14	1.3E+13	1E+14

III. Results and discussion

3.1 Energy Band diagram

The energy band diagram provided illustrates FAPbI₃-based perovskite solar cell architecture, emphasizing the electron and hole movement between the absorber, electron transport layer (ETL), and hole transport layer (HTL). In this solar cell design, the FAPbI₃ perovskite material serves as the light-absorbing layer, where incident photons generate electron-hole pairs through the process of photo excitation. The separation and transport of these charge carriers to their respective electrodes are determined by the energy band alignments at various interfaces.

The energy level alignment between the valence band maximum (VBM) of FAPbI₃ and the valence band of Cu₂O allowed seamless hole transport while preventing backflow of electrons. The band offset ensures that holes generated in the perovskite layer's valence band are injected into Cu₂O and subsequently transported to the back electrode. Cu₂O, with its favorable hole mobility and high valence band energy, not only efficiently extracts holes but also blocks electrons from recombining at the interface, enhancing the selectivity of charge transport. The Fermi level positioning at the HTL interface illustrates the split caused by photogenerated carrier accumulation, driving holes toward the Cu₂O layer and away from electrons, which are directed to the ETL [8].
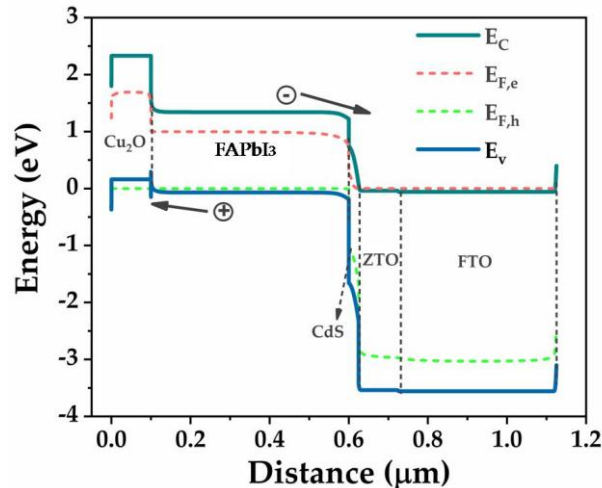
Fig. 2: Energy band diagram of FAPbI$_3$ perovskite solar cells CdS as buffer layer

On the other side, the electron dynamics at the perovskite-ETL interface are governed by the use of CdS as buffer layer. The CdS buffer layer plays a critical role in the device by improving band alignment and reducing recombination at the interface between FAPbI$_3$ and the ETL (ZTO). CdS, with its wide bandgap, prevents undesired carrier recombination and allows electrons to pass efficiently into ZTO. It acts as a selective contact for electrons while blocking holes, thereby enhancing charge separation and minimizing energy losses. Additionally, it helps suppress interface defects and stabilizes the device against degradation induced by environmental factors like moisture and oxygen. The conduction band minimum (CBM) of CdS is well-aligned with the CBM of FAPbI$_3$, creating a pathway for electrons to flow from the perovskite layer into the ETL. The sharp conduction band offset between FAPbI$_3$ and CdS acts as an energy barrier for holes, thereby ensuring that only electrons are selectively transported to the CdS layer. The CdS layer maintains continuity in the conduction band alignment and further prevents recombination losses by blocking hole leakage toward the ETL. Its optimized thickness and band structure contribute to reducing series resistance and improving charge extraction efficiency.

Within the perovskite layer itself, the spatial separation of electron and hole quasi-Fermi levels (E$_{F,e}$ and E$_{F,h}$) signifies the internal electric field established across the absorber layer. This field, driven by the built-in potential between the ETL and HTL, directs electrons and holes to their respective transport layers. The photogenerated electrons in the conduction band of FAPbI$_3$ experience a driving force toward the CdS layer due to this electric field, while the holes are directed toward the Cu$_2$O layer. This unidirectional movement ensures efficient charge separation, thereby reducing recombination losses within the bulk perovskite and at the interfaces.

3.2 Thickness Dependence of J-V characteristics

Fig. 3 (a) and 3 (b) displays the current density-voltage (J-V) characteristics analyzing the performance of a FAPbI$_3$-based perovskite solar cell with Cu$_2$O as the hole transport layer (HTL), zinc tin oxide (ZTO) as the electron transport layer (ETL), and cadmium sulfide (CdS) as the buffer layer. The plots illustrate the influence of varying thicknesses of the absorber layer (FAPbI$_3$) on key photovoltaic parameters, including short-circuit current density (J$_{SC}$), open-circuit voltage (V$_{OC}$).
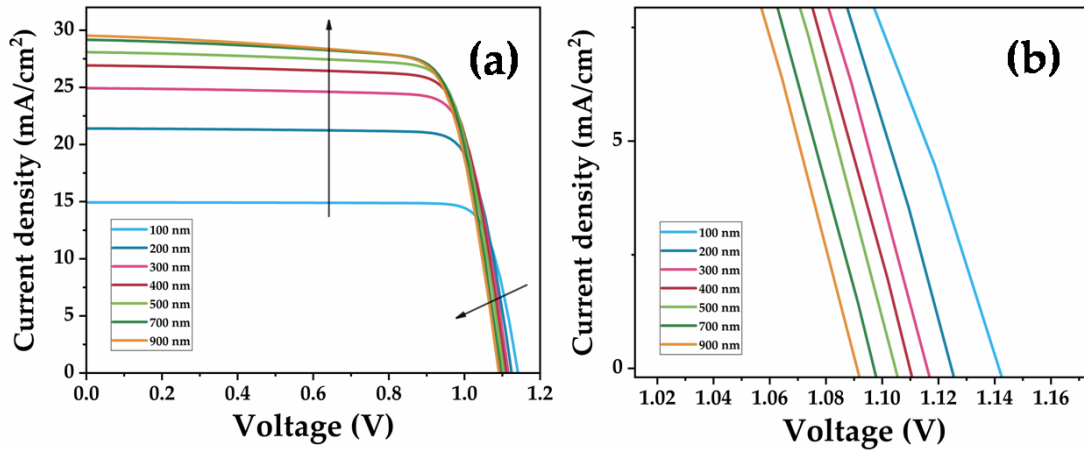
Fig. 3: (a) J-V characteristics of FAPbI$_3$ perovskite solar cell (b) Change in open circuit voltage (V$_{oc}$) with increasing absorber thickness.

Fig. 3(a) depicts the J-V characteristics under illumination for different absorber thicknesses, ranging from 100 nm to 900 nm. Thinner perovskite layers (e.g., 100 nm) exhibit reduced J$_{SC}$ and V$_{OC}$, indicative of incomplete light absorption and increased recombination losses. As the thickness increases, J$_{SC}$ improves due to enhanced light harvesting and photon absorption, resulting in greater charge carrier generation [9]. Fig. 3(b) focuses on the changing V$_{OC}$, which reveals variations in recombination rates. For thicker absorber layers, V$_{OC}$ marginally decreases due to heightened recombination at interfaces or within the bulk.

3.4 Analysis of Solar cell parameters:
Short-Circuit Current Density (J$_{SC}$)
The increase in J$_{SC}$ with absorber thickness is attributed to the improved absorption of incident photons. It is observed that the J$_{sc}$ increased from 15 to 29 mA/cm^2 with increasing thickness from 100 to 900 nm. For thinner layers, insufficient light absorption limits J$_{SC}$, as fewer photogenerated carriers contribute to the current.
Open-Circuit Voltage (V$_{OC}$)
The provided graphs in Fig. 4 (a) and Fig. 4 (b) illustrate the variation of key photovoltaic performance parameters—short-circuit current density (J$_{sc}$), open-circuit voltage (V$_{oc}$), fill factor (FF), and efficiency (η)—of FAPbI$_3$-based perovskite solar cells (PSCs) as a function of the perovskite layer thickness. The cell configuration includes Cu$_2$O as the hole transport layer (HTL), zinc tin oxide (ZTO) as the electron transport layer (ETL), and cadmium oxide (CdS) as a buffer layer.

Fig 4 (a) of the graph depicts the variation of Jsc and Voc with increasing perovskite thickness. Initially, as the thickness increases, J$_{sc}$ rises significantly due to enhanced photon absorption. A thicker perovskite layer allows for greater absorption of incident light, especially in the near-infrared region, thus generating more electron-hole pairs. However, beyond an optimal thickness (approximately 400–500 nm), the J$_{sc}$ curve begins to plateau and eventually decreases. This decline can be attributed to charge recombination effects, as the generated carriers must traverse a longer distance, leading to increased recombination losses before reaching the electrodes. Conversely, Voc exhibits a gradual decline with increasing thickness. This trend arises because thicker perovskite layers may enhance bulk recombination of charge carriers, which reduces the quasi-Fermi level splitting in the material [10].
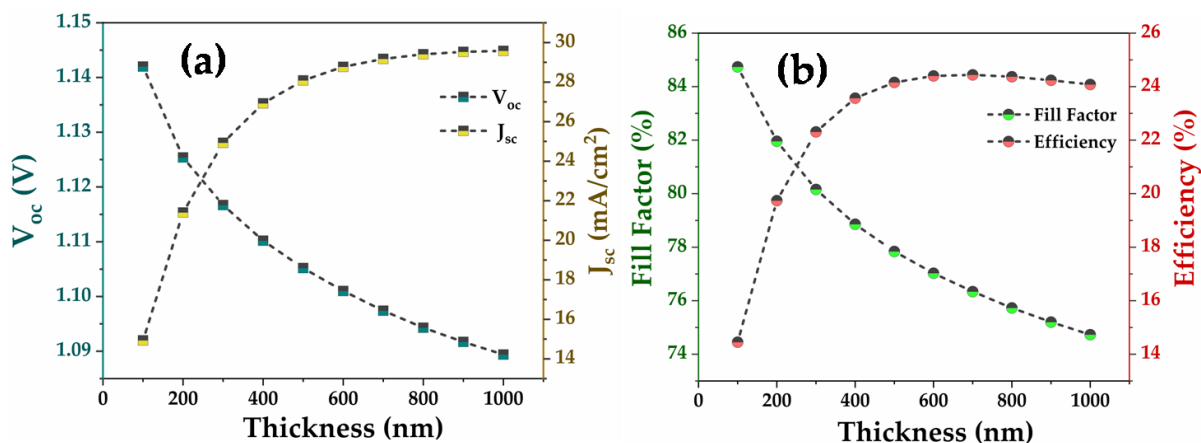
**Fig. 4 (a) Variation of Current density (Jsc) and Open circuit Voltage (Voc) with thickness.
(b) Variation of Fill factor and Efficiency with thickness.**

Fill Factor (FF) and Efficiency (η):

Fig. 4(b) provides insight into the behavior of FF and efficiency with increasing thickness. The FF initially improves with increasing thickness, likely due to enhanced carrier collection efficiencies facilitated by the greater photon absorption in the active layer. However, beyond an optimal thickness (around 300–400 nm), the FF starts to decline. The reduction in FF at higher thicknesses stems from resistive losses and increased recombination rates, which degrade the charge extraction process. A thicker perovskite layer also increases the series resistance (R_s) and decreases the shunt resistance (R_{sh}), both of which negatively impact the FF.

Efficiency follows a similar pattern to Jsc and FF. It rises steeply at first, reaching a maximum at an optimal thickness (approximately 300–400 nm), before declining at greater thicknesses. The efficiency peak corresponds to the point where the combined benefits of improved light absorption and acceptable carrier transport are maximized. Beyond this point, the detrimental effects of recombination and resistive losses outweigh the gains in photon absorption [11].

3.5 Conclusions

The performance of FAPbI₃-based perovskite solar cells strongly depends on active layer thickness, emphasizing the need for precise optimization. J_{sc} increases with thickness due to enhanced light absorption but declines beyond 400–500 nm due to recombination losses. Voc decreases with increasing thickness, reflecting greater recombination and reduced quasi-Fermi level splitting. The fill factor (FF) peaks at intermediate thicknesses (~300–400 nm), with higher thicknesses causing resistive and recombination losses. Consequently, efficiency (η) mirrors Jsc and FF trends, peaking at optimal thickness. Effective interfacial engineering, such as CdS layers, and advancements in material quality are crucial to maximizing scalability and efficiency.

References

[1] Wu, Z., Cai, H., et al. *"The tricyclic alkaloid catalyzed crystallization of α-FAPbI₃ for high performance antisolvent-free perovskite solar cells."* Energy & Environmental Science, 2024, 17, 4670–4680.

[2] Foong, J. J. Y. W., Dewi, H. A., et al. *"Enhancing FAPbI₃ perovskite solar cell performance with a methanesulfonate-based additive."* Sustainable Energy Fuels, 2024, 8, 491–495.

[3] S. Karthick, S. Velumani, J. Bouclé, et al. "Experimental and SCAPS simulated formamidinium perovskite solar cells: A comparison of device performance." Solar Energy, Vol. 205, 2020, 349-357.

[4] Lu, H. et al. "Vapor-assisted deposition of highly efficient, stable black-phase FAPbI₃ perovskite solar cells." Science 370, 74 (2020).

[5] Min, H.; Lee, D. Y.; Kim, J.; Kim, G.; Lee, K. S.; Kim, J.; Paik, M. J.; Kim, Y. K.; Kim, K. S.; Kim, M. G.; Shin, T. J.; Seok, S., "Perovskite Solar Cells with Atomically Coherent Interlayers on SnO₂ Electrodes." Nature 2021, 598, 444– 450.

[6] Mei Lyu, Nam-Gyu Park. "Effect of Additives AX (A = FA, MA, Cs, Rb, NH₄, X = Cl, Br, I) in FAPbI₃ on Photovoltaic Parameters of Perovskite Solar Cells" RRL Solar 2020, 4, 10, 2000331.

[7] Yang, L., et al. "Enhanced Efficiency and Stability of Perovskite Solar Cells Using CdS as an Electron Transport Layer." *Solar Energy Materials and Solar Cells*, vol. 176, 2018, pp. 284-291.

[8] Feng, F., Guan, Y., et al. *"Efficient additive-free FAPbI₃ perovskite solar cells achieved by promoting homogeneity."* Journal of Materials Chemistry C, 2024, 12, 3410–3417.

[9] Chen, M., Niu, T., et al. *"'Freezing' intermediate phases for efficient and stable FAPbI₃ perovskite solar cells."* Energy & Environmental Science, 2024, 17, 3375–3383.

[10] Kumar, A., Kaur, M., et al. *"Crystalline engineering of FAPbI₃ via pyrrolidinium ionic liquid for stable perovskite solar cells with 21.72% efficiency."* RSC Advances, 2024, 14, 34027–34036.

[11] Mali, S. S., et al. "CdS Buffer Layer in Perovskite Solar Cells: A Review on Material, Synthesis, and Performance." *Journal of Materials Chemistry A*, vol. 5, no. 8, 2017, pp. 3736-3747.